J. Marine. Sci. Appl. (2010) 9: 42-47
DOI: 10.1007/s11804-010-9007-y

CFD Modeling of Turbidity Current Deposition

Sergio Perez*

Department of Marine Engineering, U.S. Merchant Marine Academy, New York 11024-1699, U.S.A.

Abstract: Simulation of the flow and deposition from a laboratory turbidity current, in which dense mixtures of sediment move down a narrow, sloping channel and flow into a large tank. SSIIM CFD software is used to model 3-D flow and deposition. SSIIM predicts the height of the accumulated mound to within 25% of experimental values, and the volume of the mound to 20%~50%, depending on the concentration of sediment and slope of the channel. The SSIIM predictions were consistently lower than experimental values. In simulations with initial sediment volumetric concentrations greater than 14%, SSIIM dumped some of the sediment load at the entry gate into the channel, which was not the case with the experimental runs. This is likely due to the fact that the fall velocity of sediment particles in SSIIM does not vary with sediment concentration. Further simulations of deposition from turbidity currents should be attempted when more complete experimental results are available, but it appears for now that SSIIM can be used to give approximate estimates of turbidity current deposition.

Keywords: sediment; turbidity current; computational fluid dynamics; SSIIM; density current
Article ID: 1671-9433(2010)01-0042-06

1 Introduction

Turbidity currents are underwater flows of high sediment concentration, responsible for a range of effects of interest to geologists and oceanographers as well as civil, petroleum, ocean and environmental engineers. A high density, sediment-bearing current sinks into a body of water with a sloping bottom, and can flow for distances greater than 1 000 km, even over a flat bottom (Bruschi *et al*., 2006).

Turbidity currents are believed responsible for carving out massive underwater channels such as the Hudson Canyon near New York and the Capbreton Canyon off southwestern France (Heezen, 1956). These underwater canyons can rival in size the most magnificent canyons on the earth's surface, and must have required thousands of years to be formed. Simulations by Tetzlaff and Harbaugh (1989) for example, indicate that the Simpson Canyon in the National Petroleum Reserve in Alaska could have been formed in about 60 000 years. Simulations like those performed by Tetzlaff and Harbaugh (1989) require quite a bit of guesswork, as initial conditions such as flow volume, speed, and sediment concentration cannot be known with any certainty.

Turbidity currents operating in faster time scales, but in a no less dramatic manner, can snap submarine communication cables resting on the ocean floor. In 1929 one such event occurred in the Atlantic south of Newfoundland. An earthquake initiated a slide and turbidity current that severed cables progressively further from the earthquake epicenter for a period of 13 hours, up to 300 miles from the epicenter. From the known times of the cable breaks, a maximum current speed of about 100 km/h was calculated (Heezen, 1956), although the average speed of the current was much slower. Since then, turbidity currents have been responsible for numerous cable breaks at other locations, for example in the Mediterranean and in South America.

Underwater structures such as pipelines may also be subject to slides/turbidity currents which could cause severe damage. Recent work, sparked by ventures into very deep waters by the oil and gas industry, has focused on the hazards posed by such events, for example Bruschi *et al*. (2006), Niedoroda *et al*. (2000a, 2000b), and Reed *et al*. (2000).

Turbidity currents are also believed responsible for carrying sediments far into the oceans where only clay and oozes might normally exist. For example, a vast plain of sand and silt more than 200 miles wide exists in the Western Atlantic, probably carried by turbidity currents (Heezen, 1956).

A turbidity current emptying from a channel into an unconfined area spreads out in a depositional fan often associated with submerged hydrocarbon deposits (Tetzlaff *et al*., 1989). Heimsund (2007) used a commercial CFD package to model recent turbidity events in the Monterey Canyon, U.S.A., and the Ormen Lage Field off Norway. Salles *et al*. (2008) also simulated a recent turbidity event in the Capbreton Canyon, using a cellular automata model. Like Tetzlaff's work however, these types of simulations require guesswork of the initial conditions, as the magnitude and unpredictability of the events make it extremely difficult to gather the required input data.

Received date: 2009-03-03.
***Corresponding author Email:** perezs@usmma.edu

Turbidity currents are responsible for the accumulation of sediments on the bottom of reservoirs. This is a significant problem which requires careful attention in the design of reservoirs–accumulations can eventually render a reservoir useless, and any turbo-machinery present can become damaged by sediment particles. Currents flowing into a reservoir can carry significant amounts of sediments, particularly during floods. Numerous numerical studies of turbidity currents flowing into reservoirs have been performed; the reader is referred to Althaus for a very complete literature review.

Although numerical simulations of turbidity currents have been numerous, it appears that a simulation of a depositional fan caused by a turbidity current flowing from a channel into a large reservoir has not been verified against experiments. In this study we undertake such an effort, applying SSIIM CFD software SSIIM to experiments performed by Baas *et al*. (2004).

SSIIM is an open-source computational fluid dynamics (CFD) program for calculating sediment transport in rivers and channels, developed by faculty of the Norwegian University of Science and Technology (N.U.S.T.). SSIIM is documented in Olsen (2006).

SSIIM solves the Reynolds-Averaged Navier Stokes (RANS) equations in three dimensions. The finite volume technique is used, as well as the k-e turbulence model. The SIMPLE method is used to compute the pressure field.

The use of SSIIM for modeling sediment transport in rivers and hydraulic structures is discussed in, among others, Olsen (2006), and Ruether *et al*. (2005). In addition, SSIIM has been used to model scour around cylinders in sand, as well as sediment scour due to marine propellers (Perez and Caliendo, 2008).

SSIIM is one of several CFD tools with the capability to model sediment transport in three dimensions, among them: ECOMSED (Blumberg and Mellor, 1987), EFDC3D (Hamrick, 1992), and CH3D-SED (Spasojevic and Holly, 1994). Readers are referred to Papanicolau (2008) for a complete review of available sediment transport modeling software.

2 Simulation details

The experiment performed by Baas *et al*. (2004) consisted of a narrow, sloping channel which emptied into a large, level tank. Water covered the channel and tank, and mixtures of sediments with water were released down the channel from a mixing tank, in volumetric concentrations ranging from 14% to 27%.

The channel was 4 m in length and 0.22 m wide, and had a variable slope. Tests on coarser sand were done at a slope of 8.6°, while tests on finer sands and silt were performed at a slope of 3.7°. The tank into which the channel emptied measured 3.5 m long and 3 m in width. Tests conducted on the 8.6 degree slope were performed using a water flow rate of 7.8 L/s, while those performed on the 3.7° slope used a water flow rate of 5.2 L/s.

Sediments were mixed with the water in a mixing tank, which allowed about 15 seconds of constant sediment supply-all simulations performed in this study were allowed to run for 15 seconds of simulated time (this required about 18 hours of computation time using a laptop computer with a processor speed of 2.2 MHz).

After the 15 seconds elapsed, the sediment supply to the mixing chamber ceased, and a period of waning flow followed which lasted for about another 15~25 seconds as the mixing chamber emptied.

In the waning flow period, the flow velocity dropped fairly quickly-by about 50% five seconds after the beginning of the waning period. The concentration of the flow in the waning period was not measured by Baas and his colleagues, but was observed to decrease progressively. It is reasonable to believe that some portion of the measured accumulations of sediment in the tank were accrued during the waning period, a period not modeled in the SSIIM simulations due to lack of input data.

Three grades of sediment were used: fine sand with a mean diameter of 0.235 mm, very fine sand made of glass beads of 0.069 mm mean diameter, and coarse silt made of glass beads measuring 0.04 mm mean diameter. The sand and glass beads were assumed to have a specific gravity of 2.65 for this study; varying this density within reasonable values did not appear to alter the simulation results significantly. Table 1 details the tests conducted by Baas which were simulated in this study.

Table 1 Matrix of Simulations performed

Baas run	Sediment size /mm	Concentration /%	Channel Slope /(°)	Flow /($L\cdot s^{-1}$)
2	0.24	27	8.6	7.8
4	0.24	14	8.6	7.8
8	0.04	21	3.7	5.2
12	0.07	29	3.7	5.2

The mixture of sediment and water exit the mixing tank and flow into the channel through a gate in the mixing tank. The gate spans almost the entire width of the channel and measures 0.035 m in height. It is likely that the flow formed a vena contracta while exiting the gate, based on the drawings from Baas *et al*. (2004), but sufficient detail on the gate exit conditions was unavailable to model this accurately.

Trial simulations were performed assuming a faster flow through a smaller gate (as small as 0.6 of the original gate height, Vennard (1961), to account for the vena contracta), and did not result in significant differences in the outcome.

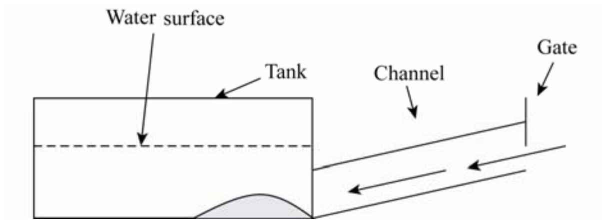

Fig.1 Test apparatus used by Baas *et al.* (2004)

A mesh with 400×30×7 grid lines was used for simulations with the 8.6° slope, while 9 grid lines were used to better resolve the slightly deeper surrounding waters at the entry conditions when a slope of 3.7° was used. The grid was finer close to the deck in order to capture details of the turbidity current. A variety of grid sizes and distributions was attempted, until a point was reached when making the grid smaller did not result in significant differences in the outcomes of the simulations.

The time step used was also tested and made progressively smaller until there were no significant differences in the outcome; yielding a time step of 0.05 seconds. SSIIM permits modifying the time step as the program runs, but the time step was maintained at a constant value.

SSIIM allows users to select from a variety methods for calculating the sediment concentration at the bed; the model by Shen and Hung (1972) gave the best results. Shen and Hung developed a regression formula based on over 500 experimental data points. Their formula requires inputs of sediment fall velocity, sediment mean size, flow velocity, and energy slope. The Shen-Hung model is known to work well in laboratory flumes and small rivers, although it appears less accurate for very large rivers (Julien, 1998).

The fall velocity of sediment particles is known to vary with concentration; particles first experience an increase in settling speed as sediment concentration increases slightly, as compared to settling speeds of single particles. However, "hindered settling", in which non-cohesive particle fall velocity is reduced, becomes evident at higher concentrations (McNown *et al*., 1952; Vanoni, 2006). Particle fall velocity is a required input to SSIMM, but it remains constant.

We found that SSIIM predicted sediment accumulation at the exit gate into the channel in all of the simulations except run 4; Baas *et al*. (2004) report that no significant amounts were seen. Simulations were performed where the fall velocity was decreased by extrapolating the results of McNown *et al*. (1952) to the high concentrations used for this study, yielding a fall velocity that is 0.63 times that of a single particle. This resulted in very little accumulation in the channel, but at the expense of reduced accumulations in the tank. Apparently a low fall velocity is required at the gate exit where the concentrations are higher, while a higher fall velocity is necessary at the channel exit where the concentrations are significantly lower. In this study, the single particle fall velocity was used, taken from Vanoni (2006).

The angles of repose of Bass's particles were measured from his results, and used as an input to SSIIM. These values were 4.8° for the 0.069 and 0.04 mm particles made of glass beads, and 10.2° for the 0.235 mm sand particles. The calculations were very sensitive to this figure–angles of repose that were too great resulted in large accumulations at the gate.

For the experiments performed using the 3.7 degree channel, Baas glued 0.235 mm sand to the channel bottom. This was accounted for in the simulations by specifying a roughness 3 times this value for the channel bottom–this is a value that has been found to give good results for simulations (Olsen, 2006).

3 Results of the sediment accumulation in the tank

Figs.2~15 show the sediment accumulation in the tank, sediment concentrations at 1.4 m from the gate, and velocities at three spots in the flow: 0.6 m from the gate, 0.46 m from the channel exit into the tank, and at 1.26 m from the channel exit.

The plots show that SSIM underestimates the size of the accumulated mound to within about 25% of the experimental values. SSIIM also underestimates the volume of the sediment mound by about 20%~50%, depending on the run modeled.

As mentioned previously, it is likely that some of the experimental accumulation occurred during the waning flow period, which was not included in the SSIIM simulation. It is then probable that the SSIIM accumulation predictions were more accurate than indicated by the results presented here.

The shape of the accumulated mound is not accurate for three of the four runs modeled; the experimental transverse sections show a double-hump that SSIIM does not reproduce. In addition, in three of the runs the location of the mound crest was inaccurate by 1.5~2 m. However, run 4, which used the lowest concentration of sand (14%), gave fairly accurate representations of accumulation geometry.

The concentration figures show that close to the deck, SSIIM predicts concentration within 2% of the experiments (3 of the runs were within 1%), but that further from the bottom the concentration values were too great by about 50% of the experimental values.

The velocities predicted by SSIIM in run 12 were off by about 0.1 m/s (out of 1 m/s) 0.6 m from the gate; while in the tank SSIIM was off by 0.2 m/s out of 0.3 m/s.

In addition, in run 2 Baas measured the flow speed at one location 0.6 m from the discharge gate. Baas gives a velocity of about 1.6 m/s, but this is obtained using a propeller meter measuring 0.025 m in diameter, with the centerline of the propeller situated at 0.03 m over the deck. The SSIIM flow velocity at 0.03 m off the bottom is 1.3 m/s, but the bottom edge of the meter's propeller would be where SSIIM's speed is about 1.9 m/s. Without running experiments on the propeller meter to determine if the reading is indeed an average reading, it is difficult to ascertain the accuracy of the SSIIM calculation. But it appears that the SSIIM values are reasonable.

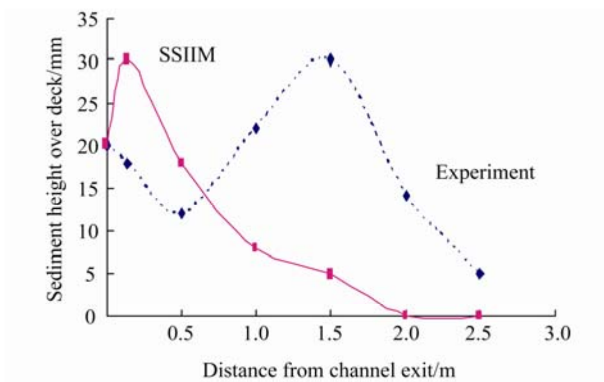

Fig.2 Sediment accumulation as a function of distance from the channel exit, Run 2 (fine sand), 14 % concentration

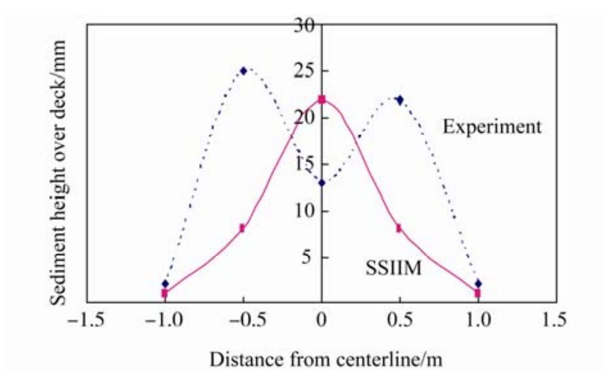

Fig.3 Sediment accumulation at the channel exit along a transverse plane, the zero point on the plot is the channel exit, Run 2 (fine sand), 27% concentration

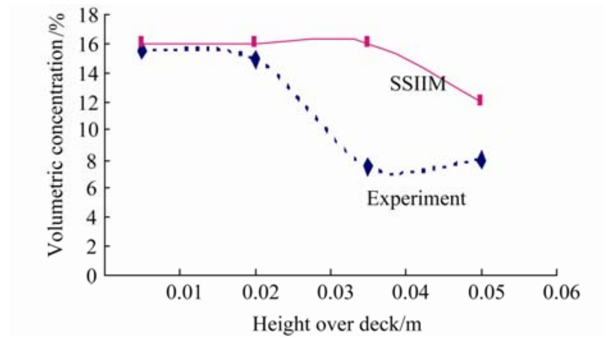

Fig.4 Sediment concentration at 1.44 m from the gate exit, Run 2 (fine sand), 27 % concentration

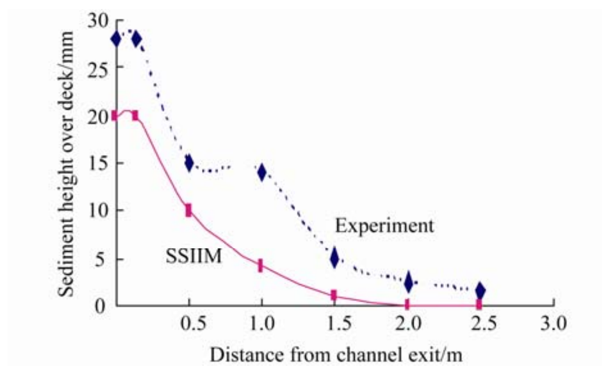

Fig.5 Sediment accumulation along a center longitudinal section as a function of distance from the exit of the channel, Run 4 (fine sand), 14 % concentration

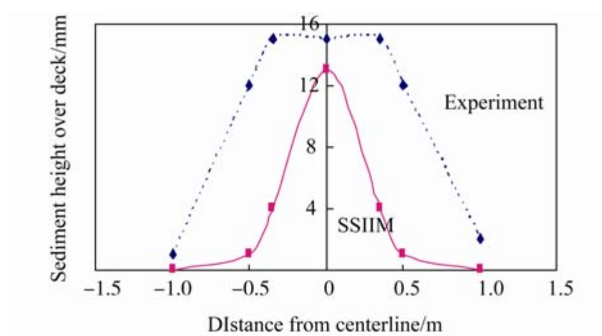

Fig.6 Sediment accumulation along a transverse section near the channel exit, the zero point on the x-axis represents the middle of the tank. Run 4 (fine sand), 14 % concentration

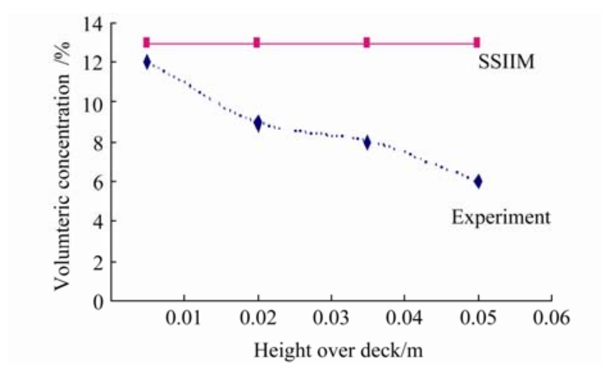

Fig.7 Sediment concentration 1.44 m from the gate, Run 4 (fine sand), 14 % concentration

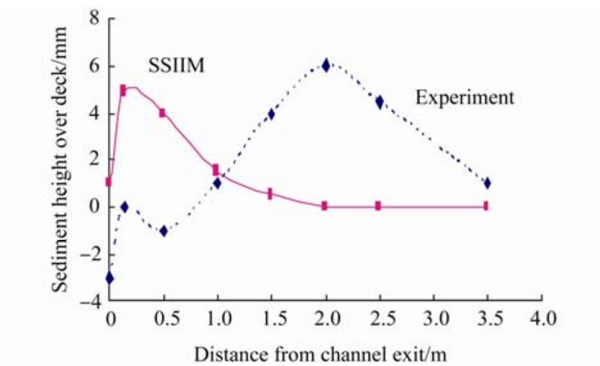

Fig.8 Sediment accumulation, longitudinal section, Run 12 (very fine sand), 29% concentration

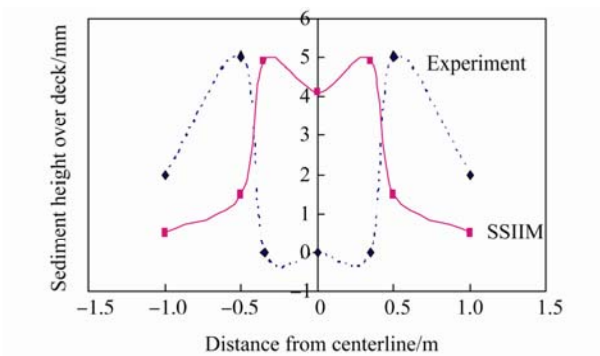

Fig.9 Sediment accumulation, transverse section, Run 12 (very fine sand), 29% concentration

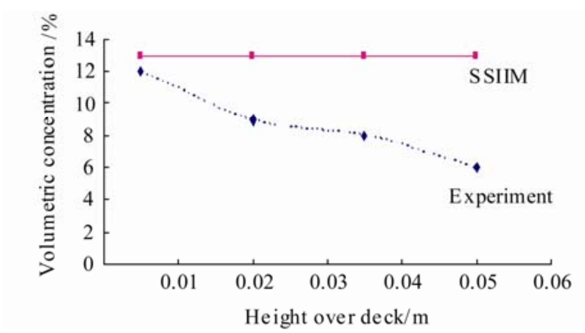

Fig.10 Concentration 1.44 m from gate, Run 12 (very fine sand), 29% concentration

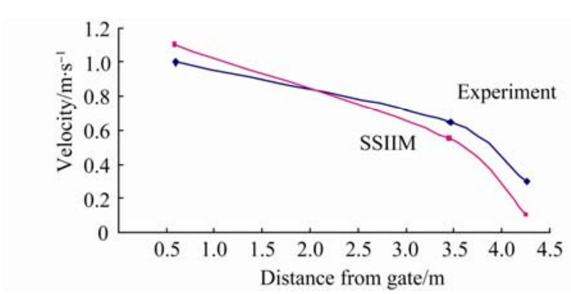

Fig.11 Velocity 0.35 m from deck, Run 12 (very fine sand), 29% concentration

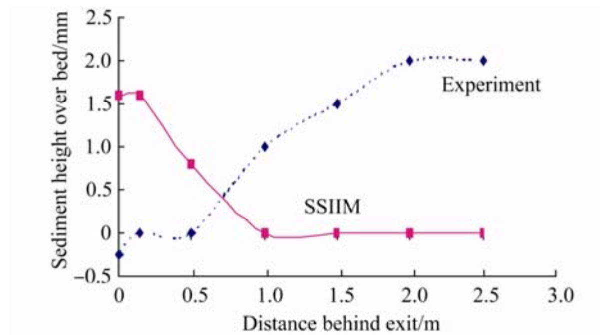

Fig.12 Sediment accumulation. longitudinal centerline, Run 8 (Coarse silt), 29% concentration

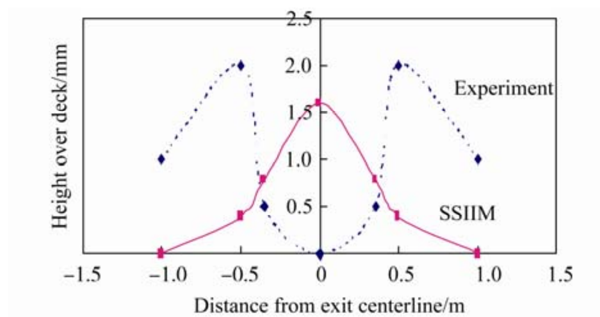

Fig.13 Sediment Accumulation. Transverse section. Run 8 (Coarse silt), 29% concentration

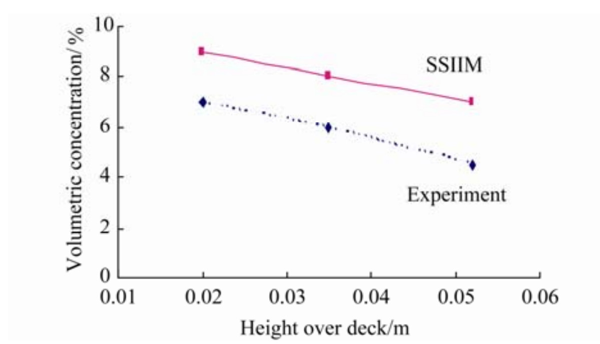

Fig.14 Sediment concentration, Run 8 (Coarse silt), 29% concentration

4 Conclusions

SSIIM underestimated the height of the depositional mound from a turbidity current by as much as 25% of experimental values, and the volume of the accumulation mound by 20%~50%. It is likely that some of this error is due to the waning flow period not specified in detail in the experimental results.

The geometry of the depositional mound is not accurate at sand concentrations greater than 14%, in which SSIIM failed to reproduce the tunnel-like cut into the mound at the channel exit, as well as the location of the mound crest.

At initial concentrations greater than 14%, the simulations dumped sediment in the channel, where little or none was present in the experiments. This is likely caused by the inability of SSIIM to vary the sediment fall velocity as sediment concentration changes.

Further simulations of deposition from turbidity currents should be attempted when more complete experimental results are available, but it appears for now that SSIIM can be used to give approximate estimates of turbidity current deposition.

Acknowledgement

The author would like to thank the Norwegian University of Science and Technology for making SSIIM an open-source program, and for providing excellent documentations for its use.

References

Baas J, Van Kesteren W, Postma G (2004). Deposits of depletive high-density turbidity currents: a flume analogue of bed geometry, structure and texture. *Sedimentology*, **51**, 1053-1088.

Blumberg AF, Mellor GL (1987). *A description of a three-dimensional coastal ocean circulation model*. In: Three-Dimensional Coastal Ocean Models, Vol.4, N Heaps, ed., American Geophysics Union, Washington D.C., 1-16.

Bruschi R, Bughi S, Spinazze M, Torselletti E, Vitali L (2006). Impact of debris flows and turbidity currents on seafloor structures. *Norwegian Journal of Geology*, **86**, 317-337.

Hamrick JH (1992). A three-dimensional environmental fluid dynamics computer code: theoretical and computational aspects. Virginia Institute of Marine Science, Gloucester Point, USA, Special Report No. 317 in Applied Marine Science and Ocean Engineering.

Heezen, BC (1956). The origin of submarine canyons. *Scientific American*, **195**(2), 36-41.

Heimsun S (2007). Numerical simulation of turbidity currents: a new perspective for small and large scale sedimentological experiments. Master Thesis, University of Bergen, Bergen, Norway.

Julien P (1998). *Environmental Sedimentation*. Cambridge University Press, Cambridge.

McNown JS, Lin PN (1952). Sediment concentration and fall velocity. *Proceedings of 2nd Mid-Western Conference on Fluid Mechanics*, Columbus, 401-411.

Niedoroda A, Reed C, Breza J, Parson B, Badalini M, Kruse G, Mullee J, Parker G, Forristal G (2000a). Developing engineering design criteria for deepwater turbidity currents. *Offshore Mechanics and Arctic Engineering Conference*, New Orleans.

Niedoroda A, Reed C, Parson B, Breza J, Forristal G, Mullee J, (2000b). Developing engineering design criteria for mass gravity flows in deep sea slope environments. *Offshore Technology Conference*, Houston.

Olsen NR (2006). A three dimensional numerical model for simulation of sediment movements in water intakes with multiblock option. Use's Manual, The Norwegian University of Science and Technology, Trondheim.

Papanicolaou AN (2008). Sediment transport modeling review–current and future developments. *Journal of Hydraulic Engineering*, **134**(1), 1-14.

Perez S, Caliendo W (2008). Calculating marine propeller scour using SSIIM CFD software. *Journal of Marine Environmental Engineering*, **9**(1), 75-84.

Reed C, Niedoroda A, Parson B, Breza J, Mullee J, Forristal G (2000). Analysis of deepwater flows, mud flows and turbidity currents for speed and recurrence rates. *Deepwater Pipeline and Riser Technology Conference*, Houston.

Ruether N, Singh JM, Olsen NR, Atkinson E (2005). 3-D computation of sediment transport at water intakes. *Proceedings of the Institution of Civil Engineers-Water Management*, **158**, 1-8.

Salles T, Mulder T, Gaudin M, Cacas M, Lopez S, Cirac P (2008). Simulating the 1999 Capbreton canyon turbidity current with a cellular automata model. *Geomorphology*, **97**(3-4), 516-537.

Shen HW, Hung CS (1972). An engineering approach to total bed-material load by regression analysis. *Proceedings of the Sedimentation Symposium*, Berkeley.

Spasojevic M, Holly FM (1994). Three-dimensional numerical simulation of mobile-bed hydrodynamics. U.S. Army Engineer Waterways Experiment Station, Vicksburg, USA, Contract Rep. HL-94-2.

Tetzlaff DM, Harbaugh JW (1989). *Simulating Clastic Sedimentation*. Van Nostrand Reinhold, New York.

Vanoni V (2006). Sedimentation Engineering. American Society of Civil Engineering, Manual No.54.

Vennard J (1961). *Elementary fluid mechanics*, *4th Ed*. Wiley Publishers, Hoboken, USA, 426.

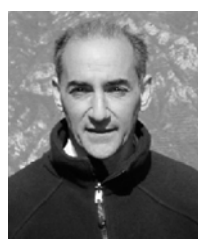

Sergio Perez was born in 1956. He is a professor of engineering at the U.S. Merchant Marine Academy. His current research interests include sediment transport and biomedicial applications of engineering.